Lateral Rotordynamic Analysis and Testing of a Vertical High Speed 12.5MW Motorcompressor Levitated by Active Magnetic Bearings

Andrea Masala[1,a], Giuseppe Vannini[1,b], Michel Lacour[2,c], Francois-MarieTassel[2,d], Massimo Camatti[1,e]

[1]GE Oil&Gas, Conceptual & Advanced Mechanical Design Dept., Florence, 50127 Italy
[2]S2M, St Marcel, 27950, France
[a]andrea.masala@ge.com, [b]giuseppe.vannini@ge.com, [c]michel.lacour@s2m.fr,
[d]francois-marie.tassel@s2m.fr, [e]massimo.camatti@ge.com

Abstract: A new high performance motorcompressor for subsea application, equipped with Active Magnetic Bearings (AMBs) from S2M, was developed by GE Oil&Gas. This paper presents the main steps of AMBs integration and rotordynamic assessment of Blue-C motorcompressor. A brief summary of acceptance test results and rotordynamic performances is finally illustrated.

Keywords: Subsea, Motorcompressor, Canned AMBs, 7-Axis Control, Rotordynamics

Introduction

To meet the needs of the growing trend toward more severe and challenging Oil & Gas industry projects, GE Oil & Gas with partnership of S2M on Active Magnetic Bearings supply has developed a hermetically sealed, high speed, high performance motor-compressor prototype for subsea applications. The Active Magnetic Bearings technology has found a natural application to meet subsea environment specific requirements because of reduced maintenance and auxiliaries system compared to conventional oil film bearings. A 7-axis controlled rotor (three radial bearings and one axial bearing) was identified as the best solution to meet rotordynamic reliability requirements during operation while a vertical rotor configuration was selected to reduce overall machine footprint, limiting subsea module weight, and reduce AMBs size and power.

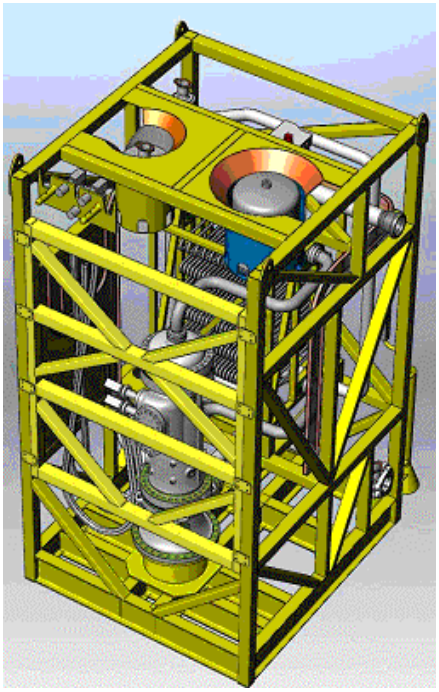

Figure 1: Compression module

Due to long run operation requirement on a subsea station, the motorcompressor was required to guarantee robust operations at different process conditions and tolerate high unbalance level, while meeting high performances in terms of power and efficiency, with 12.5 MW delivered at 11000 rpm. Since the early development phase of the project, back in 2005, AMBs integration and rotordynamic performances were identified among the main challenges of the entire project.

API 617 [1] for centrifugal compressors was selected as reference

standard for overall machine design, but rotordynamic requirement typically set for horizontal rotors supported by two oil film bearings were superseded with new criteria identified during the development phase.
As discussed by Li et Al. [3]. in addition to rotor model, the motorcompressor casing and support structure dynamics, usually not included in conventional rotordynamic analysis, was included in the rotordynamic study, to reduce the amount of uncertainties coming from system modelization.
Inputs on aerodynamic cross coupling, calculated by compressor manufacturer for several operating conditions and design parameters, were transferred to AMBs supplier to finalize controller synthesis process and target Zone-A stability requirements, as per ISO 14939-3 standard [2].
With the intent to limit the number of iterations on rotor and AMBs design, both motorcompressor vendor and AMBs supplier were responsible for separate rotordynamic unbalance and stability analysis.
To overcome the discrepancy of using AMBs synchronously reduced coefficients for stability assessment, as discussed by Swanson and Al [4], a new rotordynamic code able to integrate AMBs transfer function and perform a closed loop stability analysis according to ISO 14839-3 criteria, was developed by GE Oil&Gas.
Results in terms of unbalance response and sensitivity transfer function performed by both motorcompressor and AMBs vendor are discussed in this paper.
Starting from January 2010, the motorcompressor prototype went trough an extensive testing campaign to evaluate system performances and reliability at different operating conditions. The test allowed verifying machine rotordynamics in different load conditions and in the full speed range.
A comparison between numerical and experimental rotordynamic performances is provided in the present paper.

Rotor-Structure Modelling

Mechanical System. The motor-compressor rotor is a vertical single line rotor made of electric motor and compressor shafts. The coupling between the electric motor and the compressor shaft is made by a Hirth connection with the axial tightening load provided by a central tie bolt. The motor-compressor rotor is sustained by three radial and one axial AMBs, as depicted in Fig. 2.

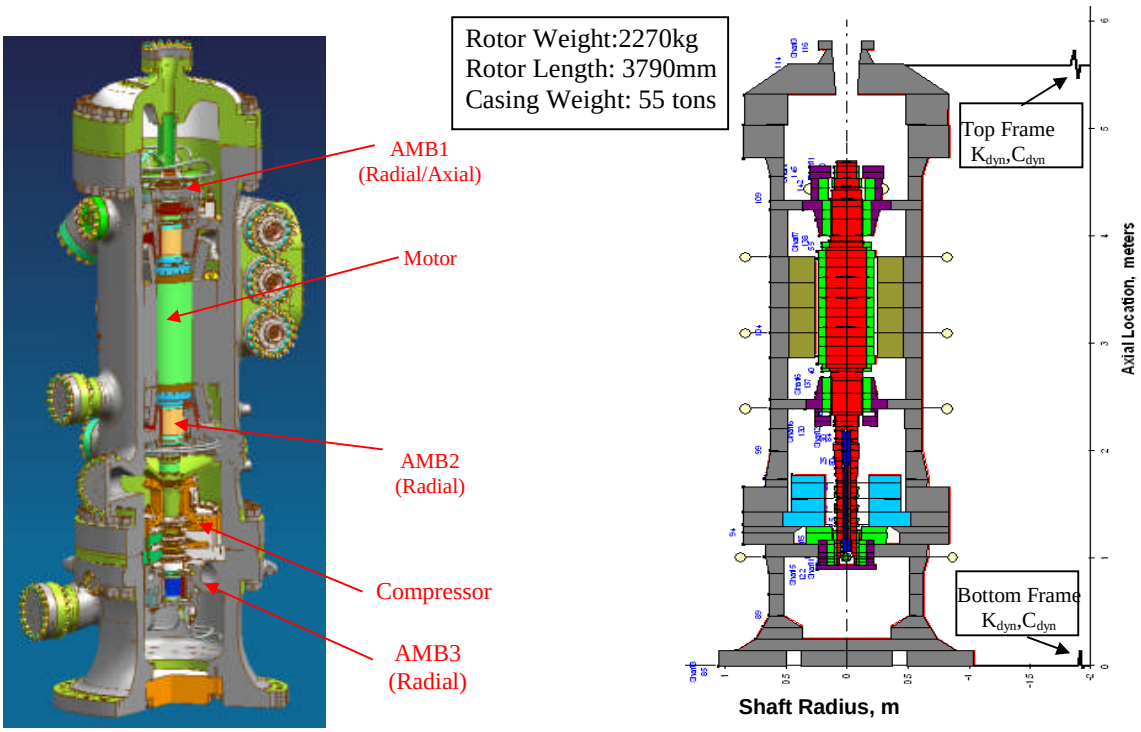

Figure 2: Motorcompressor 3D and Rotordynamic model

The rotor was modelled by means of a FEM based rotordynamic software as an assembly of two shafts, the motorcompressor rotor and the inner tie-rod, rotating at synchronous speed and connected though pinned connection at interface point.
Leveraging the symmetry of the motorcompressor casing, this was included in the model as Timoshenko beam elements, with same formulation as the rotor but with zero reference speed. Proper correspondence between 1D model and 3D casing dynamics was verified through FEM analysis and evaluated in terms of natural frequencies and mode shapes matching.
The rotor and the casing model were connected through transfer functions representing AMBs dynamics, including actuator-sensor non-collocation effects.
To account on the model the effect of the subsea frame supporting the casing, the frame structure was characterized in terms of dynamic stiffness and damping with a separate FEM analysis: both radial and bending transfer function in the 0÷2000 Hz frequency range were derived and included in the rotordynamic model as frequency dependent stiffness and damping coefficients. Top support was verified not to be effective for stiffening purpose and was finally removed.

Internal Seals Coefficients. Aerodynamic cross-coupling effects due to gas inside the machine is the main destabilizing effect in a centrifugal compressor. Dynamic coefficients for labyrinth seals on each impeller were calculated with XLlaby code [5], whereas dynamic effects due to honeycomb seal, located on the balance drum on the bottom end of the compressor, were computed with XLIsotSL code [5] for different machine operating conditions, seals clearances and geometries. Main labyrinth seals characteristics are summarized in Table 1.

	Seal1	**Seal2**	**Seal 3**	**Honeycomb**
Seal Radius [mm]	144	140	137	128
Radial Clearance [mm]	0.6	0.65	0.5	0.5
C_{eff} [Ns/m]	-0.23E3	-0.49E3	-1.47E3	1.48E3

Table 1 : Main Seals Characteristics

Special attention was dedicated to the modelling of the AMB canning, identified as potential contributors to rotor instability, due to the large surface and the high peripheral speed of the rotor facing the stator part. Both honeycomb and canning effect were introduced in the model as non-synchronous stiffness and damping coefficients applied at relevant rotor locations.

Active Magnetic Bearings. AMB actuators design was carried-out looking for a tradeoff between high load capacity requirement, both in radial and axial direction, and acceptable machine configuration and bearing span to run the machine below the 2nd bending mode. Main AMBs characteristics are summarized in Table 2.

	AMB1 (Top)	**AMB2 (Mid)**	**AMB3 (Bottom)**
Diameter, [mm]	270	270	200
Length, [mm]	220	220	150
Radial Airgap [mm]	0.8	0.8	1
Power Amplifiers Voltage, [V]	300	300	300
Power Amplifiers Current, [V]	30	30	30
Bias Current, [A]	15	15	7
Negative Stiffeness, [N/m]	1.0E+07	1.0E+07	3.6E+06
Load capacity, [N]	16000	16000	6500

Table 2: AMB characteristics

To cope with the subsea environment and target the reliability requirement, a special magnetic bearing design was implemented to protect actuator and sensor from contaminants on process gas or presence of seawater inside the machine in case of system malfunction. Corrosion resistance canning were applied both for radial and axial bearings, and as further protective action, corrosion resistance laminations were used on the bottom radial bearing, were water presence would be more likely. As a drawback of the increased corrosion resistance, the canning and laminations had the natural effect on reducing the static and dynamic capability of the AMBs which was accounted by S2M.

In Fig. 3 is represented a schematic of the AMB control loop. As practice, the details of the single components represented inside the dashed line are available only to AMB suppliers whereas only the transfer function between the displacement (y(s)) and AMB force, (F_{AMB}), for each control axis is disclosed to the OEM.

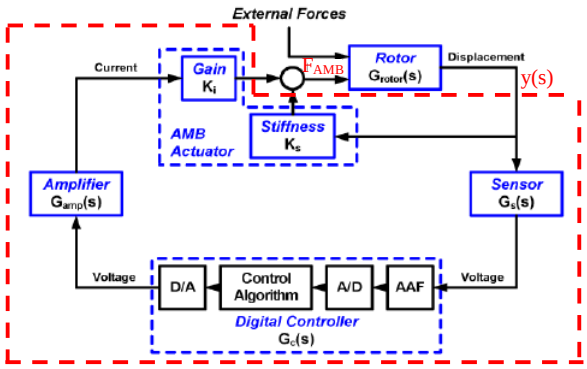

Figure 3: Closed Loop Schematic

Rotordynamic Analysis

Free-Free Analysis. To avoid critical rotordynamic issues coming from rotor 2nd bending mode crossing inside the operating speed range, the rotor was designed to keep the 2nd bending mode above machine Maximum Continuous Speed (MCS). 16% separation margin between MCS and the 2nd free-free bending mode was achieved, as depicted in Fig. 4. A margin higher than 27% was achieved when the AMB stiffness was introduced in the overall model.
Special care on the AMB controller synthesis process was paid to AMB sensor and actuator non collocation, which disturbed interlacing property on top AMB, due to a node located between sensor and actuator locations on the 3rd bending node, as depicted in Fig. 5.

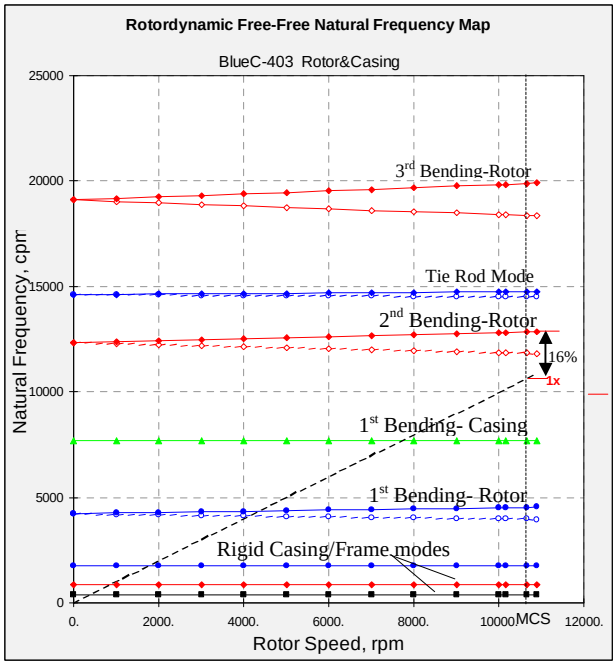

Figure 4: Free-Free Campbell diagram

Unbalance Response Analysis. Good results in terms of unbalance response vibration amplitude and amplification factor were predicted with selected AMB controller parameters. As further improvement to reject rotor unbalance, Anti Vibration Rejection (AVR), Optimum Damping Control (ODC) and Automatic Balancing System (ABS) synchronous filters were implemented in some specific speed ranges. A comparison of rotor response with 4xAPI unbalance with synchronous filters ON and OFF, is given in Fig.6.a. Benefits in terms of AMB loads are also evident in Fig. 6.b where additional margin against AMB dynamic load capacity is gained when the synchronous filters are activated.
The effect of casing and support dynamics was confirmed to be negligible in terms of unbalance response results.

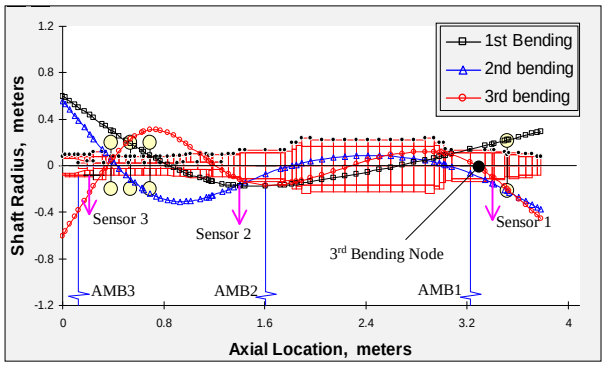

Figure 5: rotor bending modes

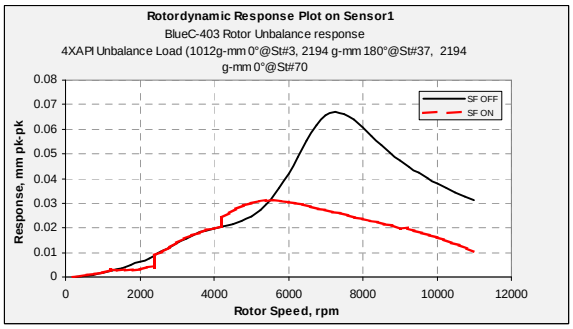

(a)

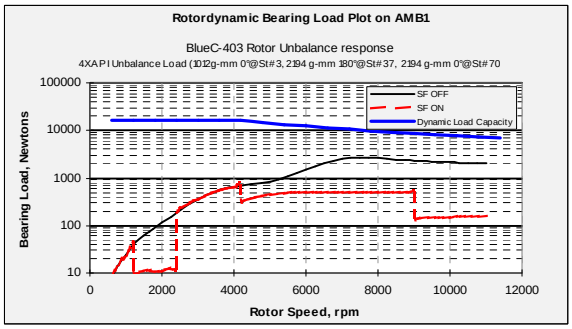

(b)

Figure 6: Unbalance response results on AMB 1

System stability System stability requirements were identified and assessed by S2M throughout control synthesis process. To perform a screening analysis among several operating conditions and evaluate system robustness at different process conditions, separate stability analysis according to ISO14839-3 were performed by GE Oil&Gas.
A new rotordynamic tool, able to integrate the rotor, AMBs and seals transfer functions in a state-space model, as represented in Eq.1 was developed to this aim.

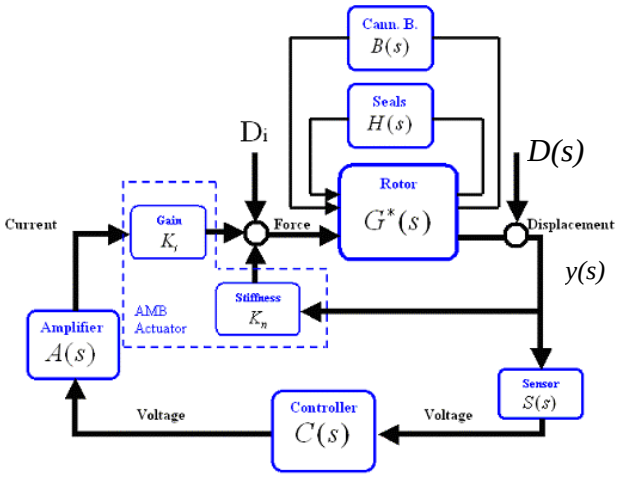

Figure 7: State space Closed Loop Model

$$\begin{bmatrix} \dot{z} \\ \dot{z}_c \end{bmatrix} = \begin{bmatrix} \mathbf{A} & -\mathbf{B_c C_c} \\ \mathbf{B_y C} & \mathbf{A_c} \end{bmatrix} \begin{Bmatrix} \dot{z} \\ \dot{z}_c \end{Bmatrix} + \begin{bmatrix} \mathbf{B_c} \\ \mathbf{0} \end{bmatrix} \begin{Bmatrix} u_e \\ 0 \end{Bmatrix}; \quad y = \mathbf{C}z + \mathbf{D}u_e \quad (1)$$

where z contains the displacement state variable x and $\dot{x}$, y is the vector of displacements measured on the sensors, u_e contains all external inputs, u_c contains the AMB control function, $\mathbf{A}$ is the dynamic matrix of the system, $\mathbf{B_c}$ and $\mathbf{B_e}$ are the input gain matrices, respectively for the control and external inputs. $\mathbf{A_c}$, $\mathbf{B_y}$, $\mathbf{C_c}$ and $\mathbf{D_c}$ are the canonical state space matrices of the AMB, derived from overall transfer function given in Eq.2. The sensitivity transfer function is calculated for each control axis as the ratio between *y(s)* and *D(s)*

$$\frac{f_{AMB}}{y} = \frac{b_1 s^n + b_2 s^{n-1} + \ldots b_{n-1} s + b_n}{a_1 s^m + a_2 s^{m-1} + \ldots a_{m-1} s + a_m} \quad (2)$$

Aerodynamic cross coupling effect was evaluated by S2M in terms of sensitivity transfer function, as depicted in Fig. 8.a. A sensitivity transfer function gain of 1.328 at 82.5 Hz was predicted on AMB1 when seals cross coupling coefficients were not included on the closed loop analysis whereas a gain 1.571 was calculated when seals effect was considered. In any case the sensitivity transfer function gain was verified to be below the Zone-A limit of 3.

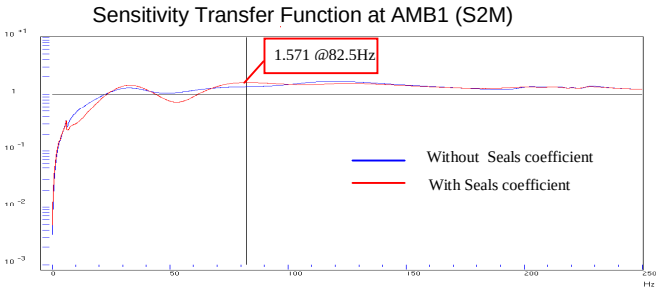

(a)

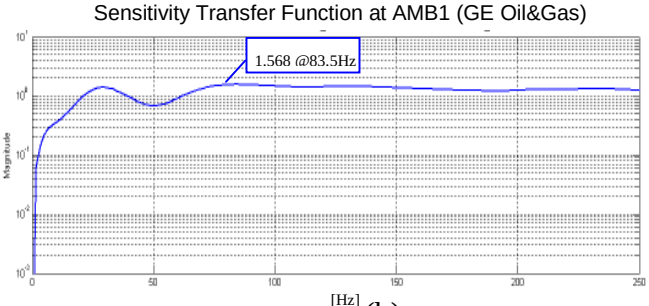

(b)

Figure 8: Sensitivity Transfer Function on AMBl

Very similar results were predicted by GE, as shown in Fig 8.b, confirming the possibility to use reduced AMB transfer function formulation from AMB supplier for evaluating system robustness in different operating conditions of the machine.

Test campaign

An extensive test was performed on Blue-C motorcompressor to assess rotordynamic and thermodynamic performances, together with system integration.
Tuning of AMBs controllers was required to reduce effects of high frequency noise and adjust synchronous filters parameters to find a optimum tradeoff between vibration amplitudes and AMBs load capability.
Vibration amplitudes were verified to be well below the acceptance limit value of 120μm both with synchronous filters on and off, as depicted in Fig. 9 (a) and (b) respectively.
Measurement of AMBs sensitivity transfer functions confirmed high system robustness level in all the operating conditions.

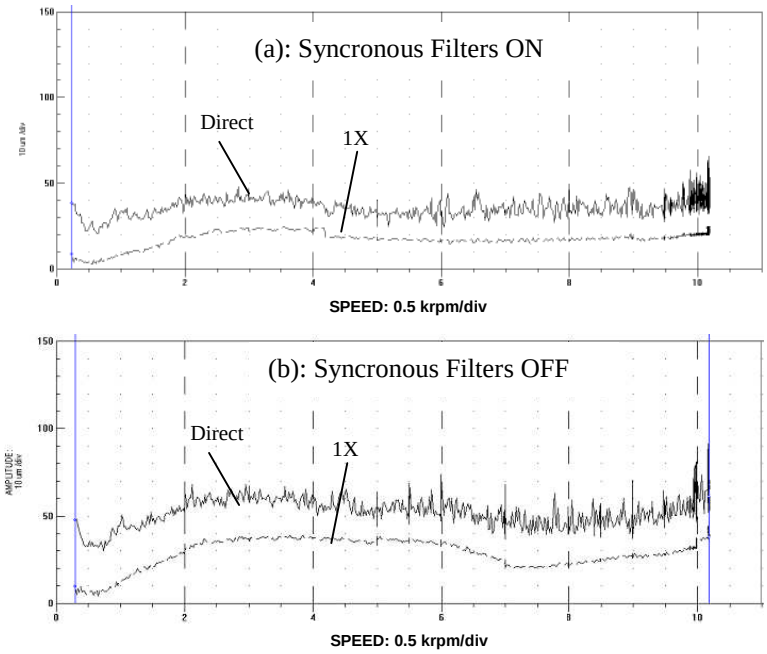

Figure 9: Pk-Pk Vibration amplitudes on AMB1 (direct and 1X component)

Conclusions

An overview of the rotordynamic studies performed on the Blue-C motorcompressor development phase is provided in the paper. The studies confirmed a need for strong integration between AMB supplier and OEM during the design of a new machines and dedicated tools to integrate specific know-how from both parties. The test campaign confirmed good rotordynamic performances and fulfilment of ISO14839 requirements.

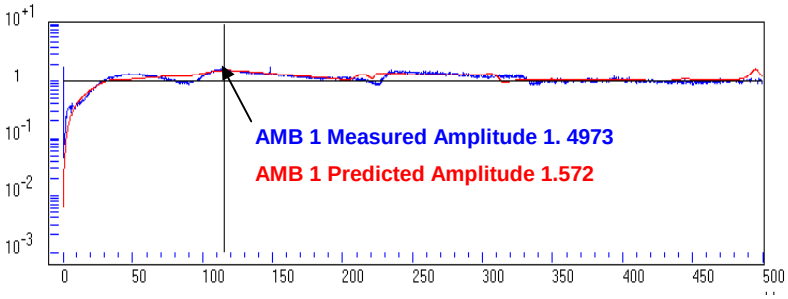

Figure 10: Sensitivity Transfer Function on AMB1 (Measured Vs Predicted)

References

[1] API 617 7th Edition, “Axial and Centrifugal Compressors and Expander-compressors for Petroleum, Chemical and Gas Service Industry”, (2002)
[2] ISO 14839 – 3, Evaluation of stability margin, (2006) .
[3] Uncertainties Classification for Rotor-AMB systems, Guoxin Li, Zongli Lin, Paul Allaire, 10th International Symposium on Magnetic Bearings (2006)
[4] Rotordynamic design audits of AMB supported machinery, Erik E. Swanson, Eric H. Maslen, Guoxin Li, C. Hunter Cloud, 37th Turbomachinery Symposium, (2008).
[5] XLTRC2 Rotordynamics Software Suite (2002): Turbomachinery Research Consortium, Turbomachinery Laboratory, Texas A&M University.